Solar Physics (2005) 229: 135–159
DOI: 10.1007/s11207-005-4721-3

PROTON ENHANCEMENTS AND THEIR RELATION TO THE X-RAY FLARES DURING THE THREE LAST SOLAR CYCLES

A. BELOV
IZMIRAN, Troitsk, Moscow region, 142190, Russia

H. GARCIA
Space Environment Center, NOAA, CO 80303, Boulder, U.S.A.

V. KURT
Institute of Nuclear Physics, Moscow State University, 119899, Vorobievy Gory, Moscow, Russia

and

H. MAVROMICHALAKI and M. GERONTIDOU
Nuclear and Particle Physics Section, Physics Department University of Athens, 15771, Athens, Greece
(e-mail: emavromi@cc.uoa.gr)

(Received 10 February 2005; accepted 3 March 2005)

Abstract. Energetic proton measurements obtained from the GOES and IMP-8 satellites as well as from ground-based neutron monitors are compared with the GOES soft X-ray measurements of the associated solar flares for the period 1975–2003. The present study investigates a broad range of phenomenology relating proton events to flares (with some references to related interplanetary disturbances), including correlations of occurrence, intensities, durations and timing of both the particle event and the flare as well as the role of the heliographic location of the designated active region. 1144 proton events of >10 MeV energy were selected from this 28-year period. Owing primarily to the low particle flux threshold employed more than half of this number was found to be reliably connected with an X-ray flare. The statistical analysis indicates that the probability and magnitude of the near-Earth proton enhancement depends critically on the flare's importance and its heliolongitude. In this study all flares of X-ray importance >X5 and located in the most propitious heliolongitude range, 15°W to 75°W, were succeeded by a detectable proton enhancement. It was also found that the heliolongitude frequently determines the character of the proton event time profile. In addition to intensity, duration and timing, proton events were found to be related to the other flare properties such as lower temperatures and longer loop lengths.

1. Introduction

Most previous works dedicated to the study of energetic proton events and their relationship to solar flares have relied upon the widely used NOAA standard for solar particle events (Garcia, 2004a). In the present study we apply the term SPE, solar particle enhancement, to emphasize the point that a broad range of near-Earth proton flux intensities is being investigated, including flux intensities well below that of the NOAA standard. Whereas, the commonly used expression for the NOAA standard is often referred to as SEP for Solar Energetic Proton event.

The first observers of the SPEs generally associated these events with solar flares. This relation was based primarily on the evident connection between ground level generally enhancements (GLEs) of solar cosmic rays (Forbush, 1946; Shea and Smart, 1990) that occurred following the onset of the great solar flares. In cases where an appropriate flare was not observed on the visible disk, indirect but convincing evidence has indicated powerful flares occurring behind the western limb. The associations between SPEs and flares were discussed by subsequent authors formulating a widely accepted belief that flares were the prima facie cause of SPEs. This concept was later challenged by Gosling (1993) and Reames (1995) who developed a new paradigm based on the concept that SPEs are the direct result of particle acceleration by CME driven shocks in the interplanetary medium. To the present time the new paradigm appears to have withstood any contravening interpretation (eg. Hudson, 1995; Hudson, Haisch, and Strong, 1995; Simnett, 2003).

The basic patterns of particle interplanetary transport and acceleration by interplanetary shocks were introduced during 1960–80s (Axford, 1965; Krimigis, 1965; Burlaga, 1967; Dorman and Miroshnichenko, 1968; Jokipii, 1971; Ma Sung, van Hollebeke, and McDonald, 1975; Gombosi and Owens, 1981). More recently, fast CMEs driving coronal and interplanetary shocks are considered by many authors to be the primary charged particle acceleration process in the vicinity of the Sun and in interplanetary space. Irrespective of the particular acceleration scenario employed, CMEs and related interplanetary disturbances are now believed to have a major influence on how the particles escape and propagate in the interplanetary medium and, consequently, what determines the SPE properties observed at Earth (Richter *et al.*, 1981; Cane, Reames, and von Rosenvinge, 1988; Kahler, 1992, 1993; Ruffolo, 1999; Berezhko, Petukhov, and Taneev, 2001; and complete references in Miroshnichenko, 2001).

However, conceding that the CME/shock interaction plays a significant role in SPE generation should not overlook the wealth of evidence connecting SPEs to flares or minimize the importance of such investigations. The result of the present work and other recent publications on the relation of proton events and flares (Balch, 1999a; Garcia, 1994; Garcia and Kiplinger, 1996; Garcia, Farnik and Kiplinger, 1998; Garcia, Greer, and Viereck, 1999; Garcia, 2004a,b) attests to the physicality of the phenomena. Clearly, the correlation between certain intrinsic flare characteristics and proton events exists, and this relationship can be, and is, used as an aid in the radiation hazard forecast process.

The various and systematic empirical correspondence between flares and SPEs provide a strong impetus to study the physics of the particle acceleration processes manifested in the form of X-rays. The majority of acceleration takes place early in the flare coincident with the release of non-thermal hard X-rays, which provide the principal analytical diagnostic of that process. Soft X-rays, our main interest in this paper, follow directly and provide the principal diagnostic for the conversion of this energy, thermalizing the mass and enabling its temperature, density, loop length, volume and total energy content to be measured (Garcia, 1998, 2000a,b). Indeed, the flare itself is, in essence, primarily a particle acceleration factory.

Van Hollebeke, Wang, and McDonald (1975) in an early effort to connect flares and SPEs used data from the Goddard cosmic ray experiment on IMP-IV and IMP-V satellites to develop a procedure for identifying the associated flare with solar proton enhancements in interplanetary space. This work summarized the properties of 125 events and demonstrated the existence of a "preferable connection region" in the range 20°W to 80°W heliolongitude.

In principle, any sporadic manifestation of solar activity, e.g., X-ray, coronograph, radio, etc., that exhibits some correlation with SPEs may be useful for the construction of proton enhancement probability models (Bazilievskaya *et al.*, 1990; Garcia, Greer, and Viereck, 1999; Balch, 1999b), however, to the present time models based on the X-ray flare have been the preferred method. A compound approach, that is with greater emphasis on non-X-ray inputs exemplified in the database http://cdaw.gsfc.nasa.gov/LWS/data/event_list.html, may prove to be more successful. The SOHO mission currently provides a space-based coronograph, EUV sensors and other solar observing instruments, which the NOAA Space Environment Center has utilized to great effect in space weather operations. Unfortunately, the SOHO time series are too short as compared with GOES data to perform long term trend analysis.

The soft X-ray flares (hereafter SXR) observed by the NOAA geosynchronous satellites have the longest continuous record for a long-term study dedicated to the relationship between flares and proton events. Two-channel soft X-ray measurements have been archived since 1974, initially by SMS 1–2 and since the end of 1975 by the GOES series. The homogenous quality of the data (the X-ray sensor, XRS, with the exception of the shift in dynamic range, has remained basically unchanged throughout this period) makes the classification of SXR flares significantly more objective than that of Hα flares. For many years the X-ray flare locations were derived from the time coincidence of Hα and X-ray flares; however, with the introduction of GOES-12 X-ray imager flare localization is possible without optical data. Soft X-ray observations also provide a means to register flares close behind-the-limb. This circumstance is very important since behind-the-limb flares are often known to be sources of the proton enhancements.

The present work is intended to be an extension of a long-term effort to define the statistical properties of SPEs and to obtain reliable indices for SPE forecasting (Kurt, 1990; Garcia, 1994; Belov *et al.*, 2001a,b; Belov, Kurt, and Mavromichalaki, 2002; Kurt, Mavromichalaki, and Gerontidou, 2002; Gerontidou *et al.*, 2002). This work has entailed a detailed selection of proton enhancements over the last three solar activity cycles (1975–2003). The main dedication of these combined studies has been to render the most probable heliographic origin of each particle event, the associated flare, its properties, and the properties of the associated proton enhancement and to place the entire ensemble into a single, unified database. This merged and enriched data set provided the basis for a new survey, encompassing recognized SPE-flare attributes with previously unrecognized or under-utilized parameters in this context. The principal objective of this work has been for the augmentation of flare-particle statistics as well as the improvement of indices for solar proton event forecasting.

2. Data

In our analysis, the integral proton fluxes (fluences) measured on board IMP-8 and GOES 5–12 satellites are used. In the earlier period 1975–1986 only data from IMP-8 have been available. At times during the 1987–2001 period, when data from the IMP-8 and GOES satellites were available, only one spacecraft's data were used because of gaps existing in the conjugate set. During the period 2002–2003 only GOES data are available.

GOES corrected integral fluxes were extracted for proton energies >10, >30, >60 and >100 MeV (see http://spidr.ngdc.noaa.gov/spidr/) as well as IMP-8 >10, >30 and >60 MeV data (see http://nssdc.gsfc.nasa.gov/omniweb/ow.html). Additionally, the IMP-8 >106 MeV/n proton and nuclear channel were also incorporated (http://ulysses.sr.unh.edu/WWW/Simpson/imp8.html). Lower energy proton fluxes were not used because of their high sensitivity to interplanetary disturbances, which tended to exhibit poor correlations with solar events. Data from IMP-8 are hourly averaged. GOES data were collected with varying time resolutions – from 1 min to 1 h. Hourly and half-hourly values of each enhancement were used to obtain estimates of the maximum and time of maximum. The difference in time resolution of IMP-8 and GOES data did not change our estimations significantly since the evolution period of an enhancement is typically much longer than 1 h even for 100 MeV protons. Moreover, the exact times of proton event onset were not required in this study, nor were other distinguishing features between IMP-8 and GOES particle data.

The X-ray flare database, based primarily on GOES observations, created by the IZMIRAN group became the basic tool for this analysis. This database has been in service for several earlier studies (Livshits, Badalian, and Belov, 2002; Osokin, Belov, Livshits, 2003). In some cases Hα flare catalogues were used to verify or to correct the X-ray flare identifications. Non-X-ray data used in this analysis included radio burst data, gamma-line measurements and CME observations from the SMM (Burkepile and St. Cyr, 1993) and SOHO satellites (see http://lasco-www.nrl.navy.mil/cmelist.html). Sudden magnetic Storm Commencements (SSC) were used as proxies for interplanetary shock arrivals and other solar wind anomalies (Belov *et al.*, 2001a,b) in order to estimate influence of the interplanetary disturbance on the near-Earth proton fluxes.

3. Proton Event Selection and Their Sources

In this work all >10 MeV and >100 MeV proton enhancements selected for study are presumed to be connected in some way with solar acceleration processes. The proton flux maximum, averaged over 15–60 min, was adopted as the main criterion of an enhancement. Proton enhancements from the IMP-8 >60 and >106 MeV channels were reckoned the equivalent of >100 MeV events by interpolation to

100 MeV. Proton enhancements with energy >500 MeV, known as GLEs (Shea and Smart, 2000), were also analyzed.

The NOAA definition of SEP events, forming the basis for the SEP catalogs (see NOAA SEC and NOAA SESC) considers the entire period of >10 pfu elevated proton flux as a single event, irrespective of the number of individual peaks occurring during the period or the number solar and interplanetary sources that may have been involved. (Note that we use the term SEP to refer to proton events meeting the NOAA criterion defined as 10 pfu sustained for >15 min, where 1 pfu is particle cm^{-2} sr^{-1} s^{-1}, which is different from the term SPE used here pertaining to >10 MeV proton enhancements on the order >0.1 pfu.) The majority of previous energetic particle catalogs were based on this NOAA/SEC definition (King, 1984; Goswami *et al.*, 1988; Feynman *et al.*, 1993; Nymmik, 1999; Mendoza *et al.*, 1997; Crosby, Aschwanden, and Dennis, 1993; Gerontidou *et al.*, 2002; Kurt *et al.*, 2004).

Since one of the main objectives of this work was to study relations between SPEs and various solar sources, we have attempted to isolate the effects originating from different sources (unlike the NOAA definition which makes no attempt to discriminate between possible sources). Therefore, in the context of the present work each proton enhancement was considered to be associated with a one particular source. An example of this is presented in Figure 1 where a series of proton enhancements are shown erupting from the active region 5747 during October,

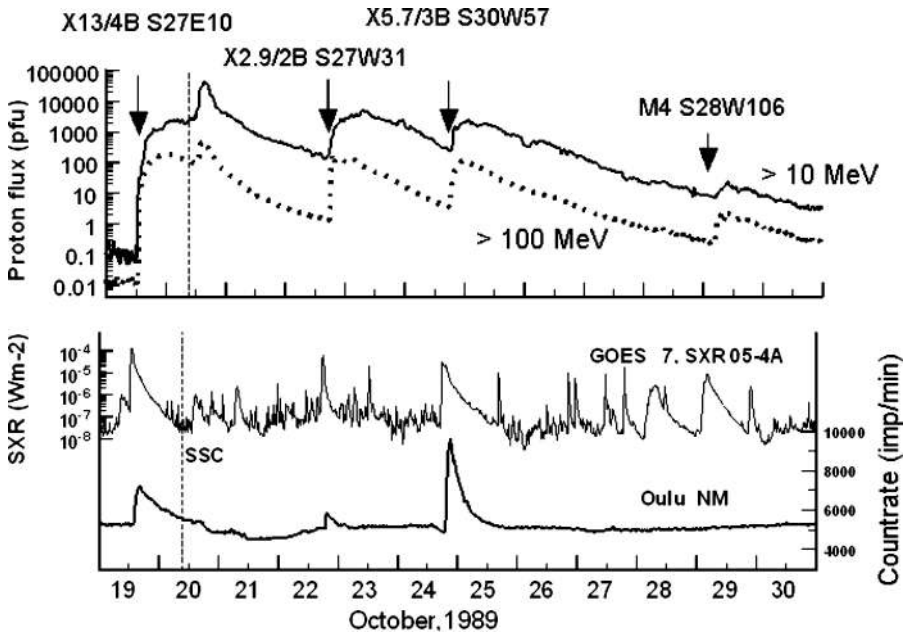

Figure 1. The example of the proton event series observed when active region 5747 passed on the disk in October 1989. GOES X-ray and proton measurements and Oulu neutron monitor data are presented.

1989. The lower panel shows three GLEs detected by the Oulu neutron monitor for the same period. Since the flux of >10 MeV protons did not fall below 10 pfu from 19 to 30 October 1989 NOAA designated the entire period as a single proton event. Of course, our adopted method makes event selections conceptually more difficult and less convenient in execution; however, it has the advantage of linking effect to cause, a notion that evidently motivated a number of earlier researchers (Van Hollebeke, Wang, and McDonald, 1974; Bazilevskaya *et al.*, 1983, 1986; Sladkova *et al.*, 1990, 1998; Cliver *et al.*, 1991).

Quiet periods made it possible to identify 10 MeV proton enhancements to 0.1 pfu, over the background, i.e., two orders of magnitude below the threshold criterion for NOAA designated SEPs. However, during very active periods when the proton enhancements followed one after another, the selection of separate proton events was much more complicated, often resulting in failure. Problematic cases of this nature usually pertain to small enhancements; however, in the case of large events discrimination was equally difficult where a new flux increases on the order 100 pfu occurred on the decay phase of the previous very large proton event. Modulation effects associated with the shocks or other solar wind disturbances also contributed to the uncertainty of selection.

Some periods experienced two or three maxima, more frequently in the case of $E_p > 10$ MeV, but sometimes occurring for $E_p > 100$ MeV particles as well. If two maxima were well pronounced and the second maximum exceeded the first, both values were included in our database, but only the first was incorporated into the numerical analysis.

Temporal proton associations with other solar phenomena play an essential role in our research. The nature of this work is that it is often subjective and generally not amenable to automatic processing. Of course, it is not difficult to associate the biggest particle flux peak or a GLE with an isolated prior occurring flare, but the problem can be manifestly more difficult if several flares occur nearly simultaneously during the period. The fast rising enhancements can be more easily connected with the individual flares as compared with gradual events.

In several instances a candidate flare for the SPE was not immediately evident. In some of these it was concluded that the source was located behind the western limb as revealed by indirect evidence: backside CMEs, radio bursts unconnected with visible solar activity and small X-ray flares unassociated with Hα flares. Apparently small X-ray flares may actually be the result of X-ray emission generated in upper part of partially occulted loops of large flares. This scenario may also be predicated on the presumed active region's recent history: that it had been visible on the disk, that it had generated a number of significant flares and that it was identified as a source of previous proton enhancements.

However, at times the selection process was conspicuously ambiguous, e.g., when two or more almost equally eligible flares were available. In order to quantify the degree of confidence of each SPE association we attributed the numerical index q_a to each proton event. The index scale ranges from $q_a = 5$, indicating a high

certainty, to $q_a = 1$, indicating no confidence. Further, the index levels $q_a = 5$ to 4 were used in all correlations and other types of phenomena - in events, where solar source characteristics were not important.

4. Data Base

The primary database for this study is contained in a new catalogue including 1144 $>$10 MeV SPE events (as defined previously), spanning over 28 years (August of 1975 till April of 2003). This number turns out to be approximately 2–3 times smaller than the number of Forbush effects and geomagnetic storms occurring in this period; it also corresponds approximately to the number (1152) of soft X-ray flares of importance $\geq$M4 in the period. The catalog also includes 547 $>$100 MeV proton events with flux intensities $I_p > 0.02$ pfu and 38 GLEs.

More than half of the SPEs (617) were identified with flares at the confidence level $q_a = 4$ or 5. Figure 2, containing the heliolatitude distribution of flares for solar cycles 21–23, shows these flares depicted as the open circles on the background of all published NOAA X-ray flares in the familiar (Maunder) butterfly form. This diagram shows that, with respect spatiality on the disc, these flares are no different from all other solar flares, irrespective of size.

Among the several flares that were missed approximately 20% occurred beyond the visible limb. Among the 151 SPEs registering $q_a < 3$ (doubtful flare association)

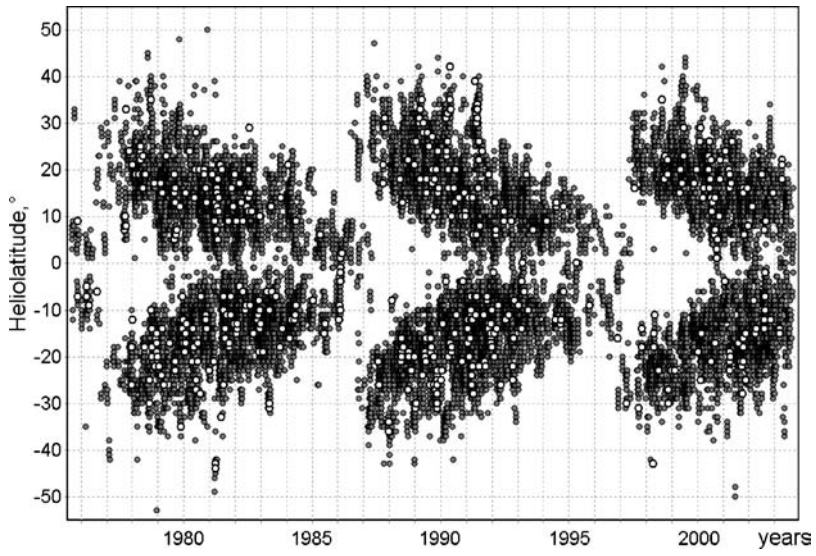

Figure 2. Butterfly diagram over three solar cycles for all X-ray flares (*filled circles*), and for the flares associated with the proton events (*open circles*).

it is likely that many were physically associated with a flare but we have no means for statistically estimating this number.

Our data base contains the main characteristics of the associated flares defined by the GOES team. The flare impulsiveness (Pearson *et al.*, 1989), determined as the ratio of the peak flux and the flare rise duration, is also given. For the ∼25% proton events the associated SXR flare temperature, emission measure and loop length were calculated (Garcia, 1998, 2000b). Additional information about type II/IV radio bursts, CME, interplanetary shock waves and some other relevant data are incorporated. Data of gamma-line measurements from the SMM GRS experiment (Vestrand *et al.*, 1999) were also included in the catalogue.

5. SPE General Properties

The following discussion describes various types of quantitative empirical relationships between the particle event and the associated flare. Firstly we discuss the features, that do not depend on the solar source identification.

5.1. SPE PEAK SIZE DISTRIBUTION

The differential distribution function $\Psi(I)$ is defined as $\Psi(I) = \mathrm{d}N(I)/\mathrm{d}I$, where $\mathrm{d}N$ is the number of events with peak value I on the interval $\mathrm{d}I$. The log-log SPE peak flux distributions are approximated by power law as indicated in Figure 3 for two energy thresholds $E_p > 10\,\mathrm{MeV}$ and $E_p > 100\,\mathrm{MeV}$. The curve fit was made for weighted values $\mathrm{d}N$ and for calculated $\mathrm{d}I_{\mathrm{mean}}$ in each log-equal intensity interval and the fitted spectral indices: $\beta_{10} = 1.37 \pm 0.03$ and $\beta_{100} = 1.47 \pm 0.06$. It

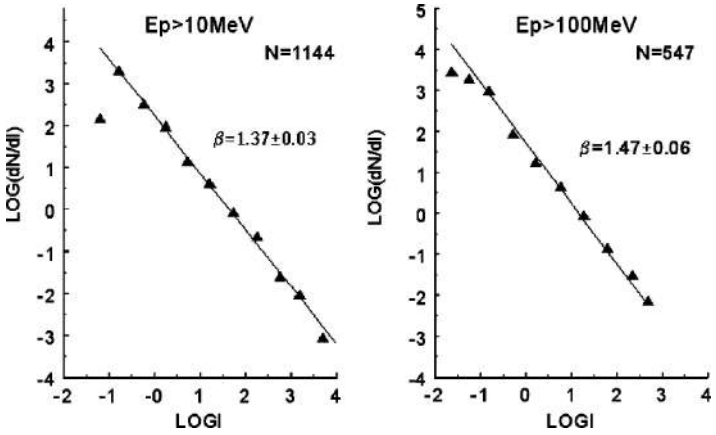

Figure 3. Peak size distribution of SPEs with energy >10 MeV (*left panel*) and with energy $E_p >$ 100 MeV (*right panel*). Lines represent the linear fitting of the weighted data.

may also be noted that various previously published spectral indices in this regard displayed significant differences in β ranging from 1.15 to 1.5 (Van Hollebeke, Ma Sung, and Mc Donald, 1975; Cliver *et al.*, 1991; Nymmik, 1999; Miroshnichenko, Mendoza, and Perez-Enriquez, 2001; Gerontidou *et al.*, 2002).

These present results are shown to be statistically more consistent as compared to those in previous works and encompass a wider peak flux interval from 0.1 to 4–6 $\times$ 10^3 pfu.

5.2. TIME DISTRIBUTION OF PROTON EVENTS

Comparing monthly values SXR flares of importance $\geq$M1 to $\geq$X3 with the monthly numbers of proton events, we obtained a maximum correlation coefficient $r = 0.743$ for the flares with importance $\geq$M5. The correlation coefficient for SPEs with monthly averaged sunspot number was noticeably smaller ($r = 0.65$). The similarity between the temporal distribution of $\geq$M5 X-ray flares and SPE numbers is evident in Figure 4 and is primarily a reflection of the activity cycle.

However, the yearly numbers of SPEs are much better connected with $\geq$M4 SXR flares (Kurt *et al.*, 2004) showing the higher computed correlation coefficient $r = 0.933$. A scatter plot of the yearly numbers of SPEs and $\geq$M4 X-ray flares is displayed in Figure 5 together with corresponding regression line.

The linear regression is apparently satisfactory for the periods with a large number of flares, but less so for small numbers, as indicated in Figure 5. In this instance a better correlation ($r = 0.947$) between flare and SPE numbers was obtained from a power law dependence: $N_{\mathrm{SPE}} = (0.79 \pm 0.07) N_{\geq \mathrm{M5}}^{0.82 \pm 0.06}$. This suggests that the number of SXR flares with importance $\geq$M4–M5 may provide a reasonable proxy index for SPE production rates (Belov *et al.*, 2001a,b).

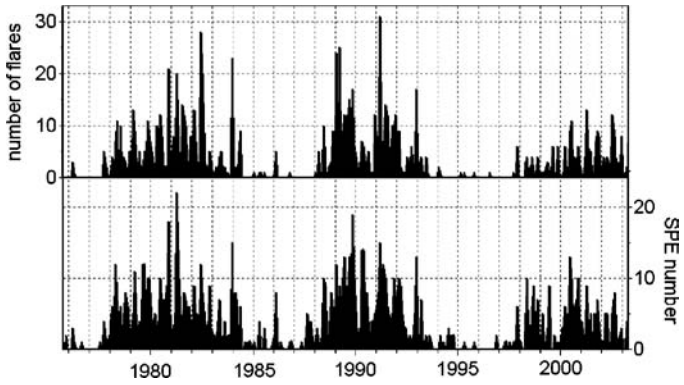

Figure 4. Monthly numbers of $\geq$M5 X-ray flares (*upper panel*), and monthly SPE numbers over the three solar activity cycles (*bottom panel*).

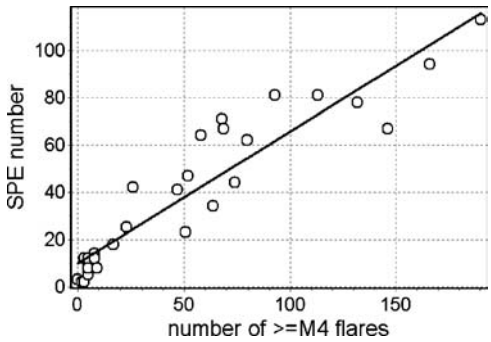

Figure 5. Scatter plot of yearly SPE numbers versus yearly number of flares with importance ≥M4.

6. Comparison of the Flare and Proton Event Characteristics

6.1. Active regions and SPEs

It is often observed that certain active regions (AR) appear to generate several proton flares in succession (see Figure 1). Not only that but the type of SPE (i.e., intensity, duration, etc.) produced by an active region often appear to bear certain similarities. Thus, the AR 5793 in November 1989 generated a series of nine SPEs in 1 week. Surprisingly, no protons with energy >100 MeV were registered in any of these events. Active regions that host a series of very powerful flares without SPEs, are very rare (assuming that the respective longitudes were favorable) as was the case in the June 1988 (AR 5047).

A common feature of active regions with a high incidence of proton flares is that the particle events themselves are usually characterized by high-energy protons. For example, the AR 6063 (May 1990) generated five proton flares with $E_p > 100$ MeV, four of which were also GLEs (except the first when this AR was situated at 38°E). Similarly, AR 6659 in June 1991 generated five SPEs with $E_p > 100$ MeV, two of which were GLEs. Among six SPEs originating from the AR 9415 in April 2001, five had proton energies >100 MeV (again, excepting the first at 31°E), and two of which were GLEs. AR 10486, responsible for the extraordinary series of flares in the October-November 2003, appears to have been most productive region in cycle 23 with ten SPEs and three GLEs.

The impression that one receives from these associations is that the ability to generate accelerated particles is inherently connected in varying degrees to the active regions. Some active regions seem to have a predisposition to proton events with energies up to 100 MeV, even 1000 MeV while others are capable of accelerations only up to a few tens of MeV. On occasion some very large active regions appear to transit the disk devoid of either large flares or SPEs.

6.2. AGE AND LATITUDE OF ACTIVE REGIONS

Protons events can be associated with new active regions in their rise phase or with old active regions, including those near the end of solar cycle. Moreover, SPE-associated flares can be originated at any latitude within the zone typical for active regions (Figure 2). Our studies also suggest that proton fluxes observed near Earth may be affected by heliographic latitude although there is not sufficient data in this regard to be statistically significant; it is observed, however, that even high latitude active regions have produced significant proton events.

6.3. LONGITUDE AND IMPORTANCE OF ASSOCIATED FLARES

The influence of heliographic longitude on the probability that a SPE may be observed near Earth is well known and well documented (Bazilevskaya and Sladkova, 1986; Cane, 1998; Belov *et al.*, 2001a,b). A strong heliographic longitudinal dependence of GLEs is also well known (Shea, 1990). First, we consider this topic in the context of >10 MeV proton events.

A scatter plot of SXR flare maximal flux versus longitude with and without SPEs over 3 solar cycles is demonstrated in Figure 6 for major flares. The SPE associated flares are depicted by filled circles. There is a conspicuous lack of SPEs in the case of eastern and relatively weak flares (left lower corner of Figure 6). In contrast, the majority of intense western flares are SPE flares. The region containing a high percentage of SPE flares extends to the center of the disk, gradually diminishing eastward for the more powerful flares. Thus, all flares with importance $\geq$X7 and longitudes west from 45°E were followed by proton events (upper right part of Figure 6).

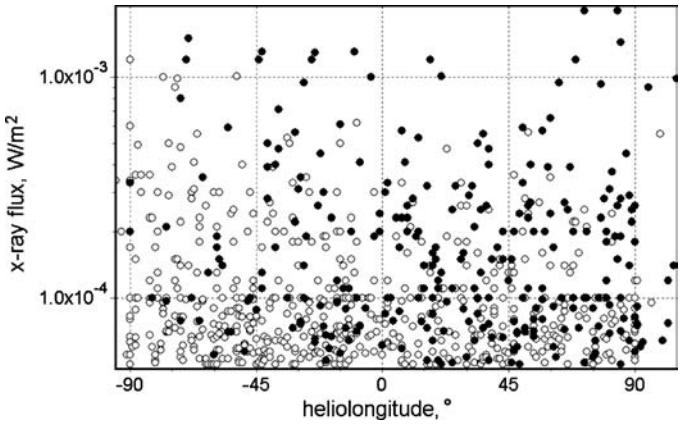

Figure 6. X-ray flare maximum flux versus flare heliolongitude. The flares associated with >10 MeV protons are depicted by the *filled circles* and others – by the *open circles*.

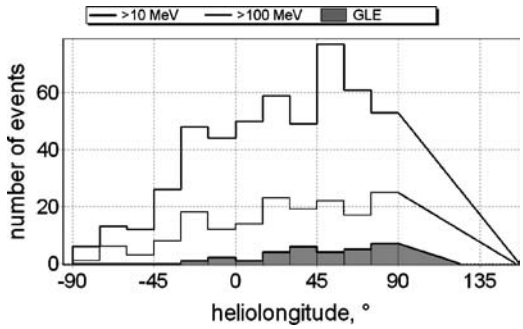

Figure 7. Longitudinal distributions of the SPE associated flare numbers. Distributions are given for flares associated with >10 MeV, >100 MeV SPEs and GLEs.

6.4. LONGITUDINAL DEPENDENCE

The number of SPE associated flares in each 15 degree heliolongitude interval was determined for each of the following SPE energy ranges: $E_p > 10$ MeV, $E_p > 100$ MeV ($I_p > 0.01$ pfu) and GLEs. Since the exact location of behind-the-limb flares was unknown they were included collectively in the most western longitudinal bin. The number events $n(\varphi)$ was assumed to decrease linearly with longitude in the range of 75°W–90°W to zero at the longitude φ_u. The upper limit of φ_u was defined by the integral $\int_{90}^{\varphi_u} n(\varphi)\,d\varphi$ required to be equal to the total number of the sources behind the limb. The resulting longitudinal SPE distributions for energy >10 MeV, >100 MeV and GLEs is presented in Figure 7.

It is seen that a 30°E demarcation heliolongitude is the eastern limit for GLE associations. The 30°E heliolongitude is also significant for >10 MeV and >100 MeV protons. The great majority of proton flares were located within the longitude interval 30°E–120°W (97% for GLEs, 96% for $E_p > 100$ MeV and 94% for $E_p > 10$ MeV); these results are also consistent with Van Hollebeke, Ma Sung, and Mc Donald (1975); Bazilevskaya and Sladkova (1986); Belov *et al.* (2001a,b). Variations of $n(\varphi)$ are relatively moderate within this longitude range with the notable exception of >10 MeV SPEs in the 45°W–60°W interval. The GLE and >100 MeV distributions remain high to the western limb.

The maximum of $n(\varphi)$ distribution for >10 MeV SPEs in the 45°W–60°W interval seems to be not accidental as these longitudes also coincide with the approximate location of footpoints of quiet solar wind interplanetary magnetic field lines connecting the Sun and Earth. For solar wind speeds of 300–700 km/s these IMF lines span a wider longitudinal range of 25°W–75°W, which also overlaps the greater part of the SPE source longitudes. The proton trajectories are sometimes known to cross into the near Earth connected field lines from the neighboring longitudes, especially from the west. Our longitudinal distribution plots show that SPEs associated with flares westward of 70°W have a remarkably high probability of being

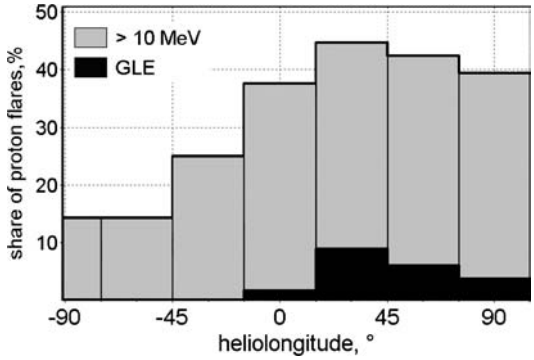

Figure 8. Longitudinal distributions of associated flare fractions in the M8/X3 flare importance interval. The distributions are given for flares associated with >10 MeV protons and with GLEs.

registered at Earth. It is also to be noted that 10 of the 38 GLEs examined here were associated with behind-the-limb flares.

The SPE probability for the most representative flare importance range M8–X3 in dependence on longitude is illustrated in Figure 8.

Protons have a vastly greater chance to be recorded near Earth after the western flare. This applies to both relativistic and relatively low energy (∼10 MeV) protons, however, in the latter case the longitudinal distribution of the sources is generally broader than for the GLEs.

6.5. Mean time profiles of SPEs

The epoch method was applied separately to three SXR flare sets, with and without protons, using proton flux time profiles measured by IMP-8. The X-ray flare onset of each event was used to mark zero time. All available proton data without gaps were used over the next 40 h. The results of our calculations for proton fluxes with $E_p > 10$ MeV and $E_p > 60$ MeV are set out in three panels of Figure 9.

Averaged proton flux time profiles from the 42° western (0°W–90°W) flares with importance ≥M5, are presented in the upper panel. The averaged proton fluxes are seen to commence soon after flares onset and achieve maximum values of 400 pfu within 20 h for $E_p > 10$ MeV and 80 pfu within 10 h for $E_p > 60$ MeV.

The middle panel depicts proton fluxes averaged over 939 flares located in the same longitude interval but with weaker importance C1-M1. In this case the proton flux enhancement become noticeable about 3 h after the flare onset and maximum fluxes do not exceed 10 pfu for $E_p > 10$ MeV and 1.5 pfu for $E_p > 60$ MeV.

The third set consists of 19 powerful eastern flares (0°E–70°E) with importance ≥M5. The results for this set are presented in the lower panel of Figure 9. There is no distinct enhancement in the proton fluxes following the flare for either the

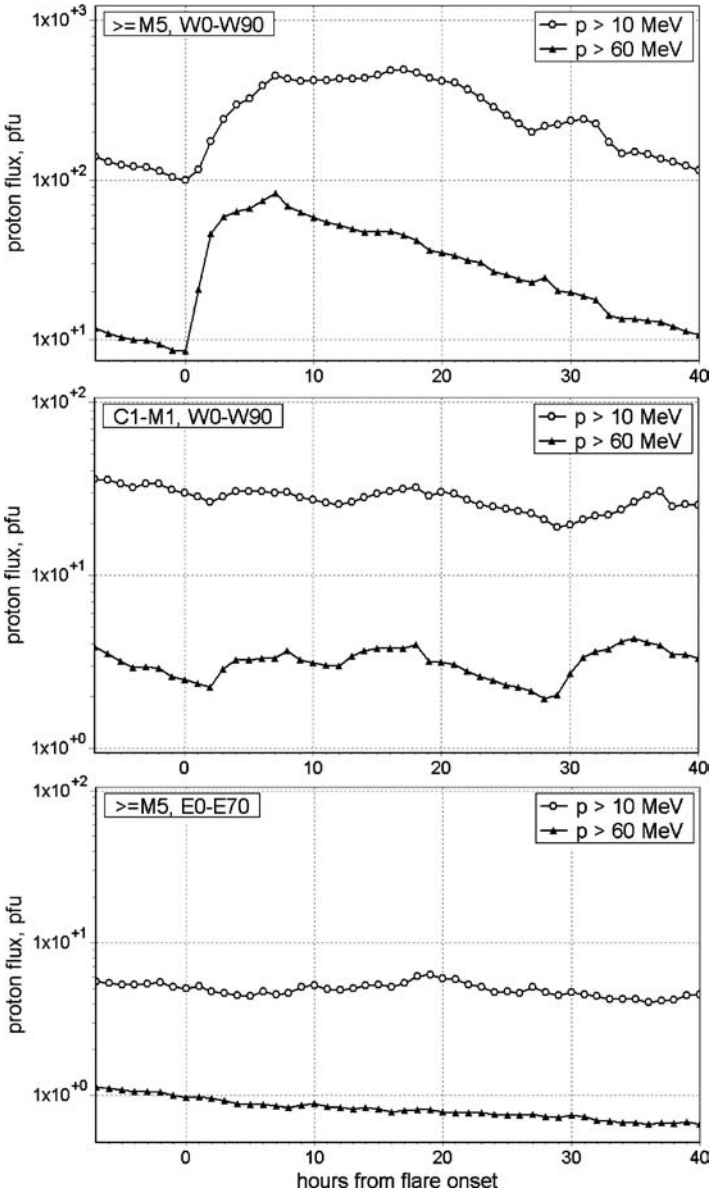

Figure 9. Mean proton flux time profiles obtained by epoch method for proton energy >10 MeV and proton energy >60 MeV (IMP-8 data) in the time of different X-ray flares.

>60 MeV or the >10 MeV energies. It is noteworthy that in all of these selected sets the proton enhancements occurred on elevated proton backgrounds caused by previous events. The fact that the flares often occur in series is a serious shortcoming in the epoch method.

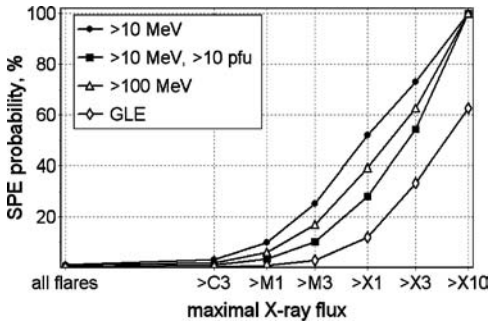

Figure 10. Dependence of SPE probability on X-ray flare importance. All >10 MeV proton events are depicted by *filled circles* and events with proton flux > 10 pfu by *filled rectangles*; >100 MeV proton events are presented by *open triangles* and GLEs by *diamonds*.

Thus, we see that the mean proton enhancement after major western flares is very large and far above the threshold of class II radiation storms as defined by the NOAA/SEC classification system (*http://www.sec.noaa.gov*). The mean proton enhancement following weak, easterly flares is an order of magnitude smaller.

6.6. Flare importance and SPE probability

The SPE probabilities (percent) of associated SXR flares for different importance thresholds are calculated and presented in Figure 10. To avoid the longitudinal dependence, only central and western flares (i.e., located west of 20°E) have been used.

It is evident from this figure that the SPE probability first becomes noticeably significant in flare importance range of C3-M1. One out of four X-ray flares of ≥M3 importance results in a measurable level of >10 MeV protons. At importance ≥X1, more than half of flares have measurable >10 MeV protons and GLE incidence becomes significant. Proton incidence and flux increases sharply above this level of importance. Among the 24 flares with importance >X5 only four were not followed by SPEs (though some were perhaps impeded by an unfavorable AR longitude). In this sample the highest registered intensity flare not associated with protons, X6.2, occurred on December 13, 2001 in the eastern hemisphere (N16E09).

At a slightly higher flare importance, >X6.5, averaged SPE flux levels increased substantially; SPEs associated with all 14 flares, occurred to the west of 20°E, exhibited elevated flux levels (≥30 pfu); nine of these flares were followed by GLEs. All 8 suitably located flares of >X10 importance in this sample were followed by proton enhancements up to >100 MeV levels; the majority of these events also registered as GLEs. As a rule for >X10 flare associations >10 MeV proton peak fluxes exceeded 1000 pfu; in only two such cases did the SPE not exceed 100 pfu.

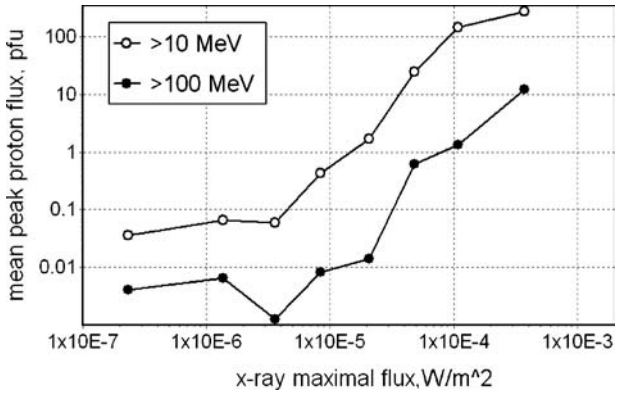

Figure 11. Mean SPE peak fluxes versus X-ray flare peak flux averaged over all X-ray flares.

6.7. Flare importance and SPE peak flux

Figure 11 shows the dependence of mean proton maximum flux on the X-ray flare peak flux. All X-ray flares (flares with and without proton associations, western and eastern flares and flares without optical identification) were used for these calculations. SXR flares were sorted according to equal logarithmic intervals in their maximum flux, dI_x. The averaged I_x value was then determined as well as the averaged proton flux, I_p, in each dI_x interval of X-ray emission.

In all of the above categories the mean proton fluxes were sufficiently high in the range 0.001–100 pfu. On average, according to the NOAA classification system, a solar radiation storm, level I, occurred following an X-ray flares of importance ~M5 and a moderate radiation storm, level II, occurred following a ≥X1 flare.

Averaged X-ray flux I_x and averaged proton flux I_p for each interval dI_x were also calculated for the cases with well-associated flares. These results are presented in Figure 12. Longitudinal effects were minimized in this part of the study by only employing flares within the relatively narrow longitude interval 15°W–75°W. Peak proton fluxes were expressed in terms of peak X-ray fluxes according to the following relation: $I_p(>10\,\mathrm{MeV}) = (4.8 \pm 1.3)10^7\ I_x^{1.14\pm0.14}$, and $I_p(>100\,\mathrm{MeV}) = (2.6 \pm 1.1)10^6\ I_x^{1.19\pm0.22}$, where I_x is measured in W/m^2, and I_p in pfu.

6.8. Time delay between flare onset and the SPE peak flux time

The distribution of >10 MeV SPE peak flux time delays, $\Delta t = t_{\max} - t_0$ relative to the SXR flare onset time t_0 is presented in Figure 13.

The main peak of this distribution occurs between 2 and 10 h with the highest concentration of events for delays of 3–4 h. Minor subpeaks in the distribution are observed but the general trend is monotonic to 70 h of delay. This wide distribution

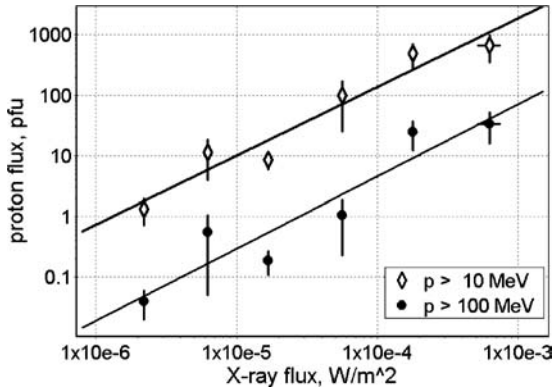

Figure 12. Mean SPE peak fluxes versus X-ray flare peak fluxes averaged over associated flares.

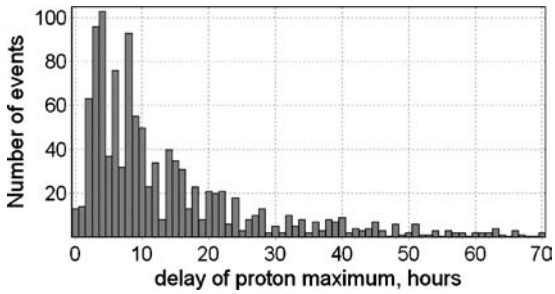

Figure 13. Distribution of the time delay between associated X-ray flare onset and SPE maximum.

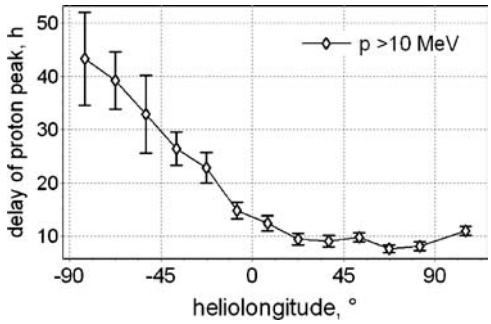

Figure 14. Averaged SPE peak time delay dependence on the longitude of the associated flares.

may be attributed primarily to different source longitudes as demonstrated in Figure 14, which empirically quantifies time delay as a function of heliolongitude.

These data were obtained by averaging the time delays of >10 MeV protons, t10, binned according to longitude intervals. The shortest delays, i.e., fastest particles, originated approximately between 60°W–90°W longitudes. Averaged behind-the-limb origin SPE time delays (assigned to the 105W longitude bin) were slightly higher than the 60°W–90°W sector and approximately equivalent to delays in the

15°W–60°W sector. Time delays for eastern flares increase monotonically (and almost linearly) from the central meridian eastward. Nearly half of all eastern SPEs (48.3%) had time delays of >20 h, whereas western (0°W–90°W) SPEs with >20 h delay did not exceed 8%. However, a small fraction of large delay events did occur even in the most favored longitude sector; viz., 5 SPEs, among 72 selected events, had delays of >16 h among in the longitude range 35°W–85°W.

These data also suggest that heliolatitude λ (or difference $\Delta\lambda = \text{abs}(\lambda - \lambda_E)$ between the solar source and the Earth heliolatitudes), may also have an effect upon SPE delays. In all of the above five large delay events in the 35°W–85°W longitude sector $\Delta\lambda > 20°$. None of the remaining 38 events with $\Delta\lambda < 20°$ shown had large delays.

6.9. Effect of the interplanetary propagation

In view of the strong heliographic influence (mostly longitude) upon SPE time delays it is reasonable to consider what effect spatiality and directivity have on the different diffusion modes on the propagating particles from Sun to Earth. In short time delay events clearly parallel diffusion is dominant, in long delay events propagation is controlled by perpendicular diffusion. In those few cases when large delays are not easily explained by either longitude or latitude effects, it is necessary to suppose the existence of some special conditions in the Sun–Earth vicinity, such as CMEs and coronal holes, (Kunches and Zwickl, 1999).

The latter point is demonstrated by many examples, particularly in the case of strong flares, i.e., ≥M6 importance, located in the longitude interval 0°W–75°W. In each of 17 cases with a large flare, shocks (undoubtedly connected with the preceding flare) were registered near Earth (with time delay <10 h). Only two of these events (<12%) were proton enhancements recorded at Earth with maximum delay less than 10 h relative to the flare onset. In cases without shocks, 67 out of 234 flares (29%) were followed by SPEs with a fast maximum. Interplanetary shocks (and IMF disturbances) arriving at Earth simultaneously with the solar particles appear to have prevented the fast evolution of the SPE, and may have at times caused the SPE to be unobserved (e.g., the gamma-ray flare in August 1989). Obviously, the influence of interplanetary conditions on the SPE evolution comes in a great variety of forms; moreover, it creates a serious handicap for the study of SPE links to the solar source. The main impediments to interpretation encountered during this work were due to the inhomogeneity of interplanetary conditions and the related problems of particle propagation.

7. Relation to Other Flare Properties

As previously demonstrated, the probability of SPE occurrence increases with the X-ray importance of the associated flare. Additionally, delays and other temporal

TABLE I

Mean properties of the associated flares and the flares without protons in the longitude interval 20°E–90°W.

Characteristic of flare	Proton flares	Flares ≥M6 without protons
Number of events	409	162
X-ray intensity (Wm^{-2})	$(1.16 \pm 0.11)\ 10^{-4}$	$(1.16 \pm 0.06)\ 10^{-4}$
Duration (min)	80 ± 4	57 ± 4
Rise time (min)	21.5 ± 1.4	15.0 ± 1.9
Heliolongitude (°)	37.5 ± 1.5	29.7 ± 2.4
Latitude difference ($\Delta\lambda°$)	17.5 ± 0.4	19.4 ± 0.7
Temperature (10^6 K)	17.7 ± 0.4	19.9 ± 0.3
Loop length (10^3 km)	37.9 ± 2.0	22.9 ± 1.4
Impulsiveness ($10^6\ Wm^{-2}\ min^{-1}$)	13.7 ± 1.7	19.2 ± 2.2

behavior of SPEs are shown to be strongly dependent on the heliographic location of the source. In this section we compare the other soft X-ray flare characteristics including the duration, X-ray loop length and maximum temperature derived from a large flare sample, 1976 to 1996 (Garcia, 2000b). We have also added the flare's impulsiveness (Pearson *et al.*, 1989) to this set.

The characteristics provided in Table I were considered for 409 flares of ≥M6 importance (X1.2 average) in the 20°E–90°W longitude range. For comparison, the characteristics of SPE-less flares are juxtaposed with those of SPE flares in the same longitude interval. In both sets the average flare intensity turned out to be X1.2.

Table 1 shows several notable differences between SPE and non-SPE flares. On average: SPE flares are situated closer to the foot points of magnetic fields that are well connected with the Earth. SPE flares have lower impulsiveness, longer duration (both rise and decay times), lower temperatures (Garcia, 2000a) and longer X-ray loops (Garcia, 2000b) as compared with non-SPE flares.

7.1. Duration of the flare and SPE probability

The averaged SPE associated flare duration is 1.3 h. That is almost 40% longer than the averaged non-proton flare. In order to construct a more detailed correlation function between SPE probability of occurrence and flare duration, all flares within the broad 20°E–90°W longitude sector were binned into two principal intensity classes: low <M6 and medium M6-X3 (>X3 flares were also investigated but not included because of insufficient statistics), and four duration classes: <30 min, 31–60 min, 61–90 min, >90 min.

The results (with error bars) are presented in Figure 15. The dependence of SPE probability on the flare duration is clearly evident. In the weakest (<M6) group the

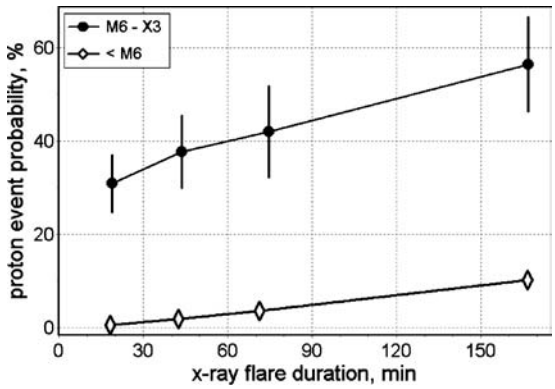

Figure 15. Proton event probability dependence on SXR flare duration calculated for two SXR flare ranges (<M6 and M6-X3) in 20°E–90°W longitudes. The statistical error for lowest flux range <M6 is smaller than the point size.

SPE probability increases by a factor of twenty for longest flares as compared with the impulsive ones. SPE probabilities were the highest for the most intense flares, >X3 (not shown) but were apparently independent of flare duration. However, in the latter case two caveats must be considered: firstly, as noted, importance >X3 flares were not considered in this analysis because of poor statistics; and secondly, many extreme flare durations exceeded the cutoff criterion used in GOES catalogues (Garcia, 2000a).

7.2. Temperature and loop length

Garcia (1994) found that SPEs correlate with low-temperature flares across the flare intensity spectrum. We considered the same flare groups as in preceding paragraph to investigate possible relationships between the SPE probability, maximum flare temperature, T_m and the length, L, of X-ray loop. (Loop length, L, used in this analysis, is a computed quantity empirically derived from measured loops, temperatures, rise and decay times obtained from soft X-ray observations, Garcia, 2004b.) The present study found little correlation between T_m and L. However, Figure 12 in Garcia (2000a) shows a monotonic decrease in temperature with increasing loop length. Here we treat T_m and L as independent parameters in order to demonstrate the relative magnitudes of influence of T_m and L on SPE incidence as shown in Figure 16. Since virtually all of the 24 events from the group ≥X3 with calculated T_m and L were also the proton events, this group was excluded from this part of the study. Two remaining groups, <M6 and M6-X3, were divided into several subsets according to temperature and loop length, with an attempt to obtain approximately equal numbers in each. To accomplish the latter the M6-X3 bin matrix consisted of three temperature columns, $T_m < 17$ MK, $T_m = 17$–21 MK and $T_m \geq 21$ MK; and

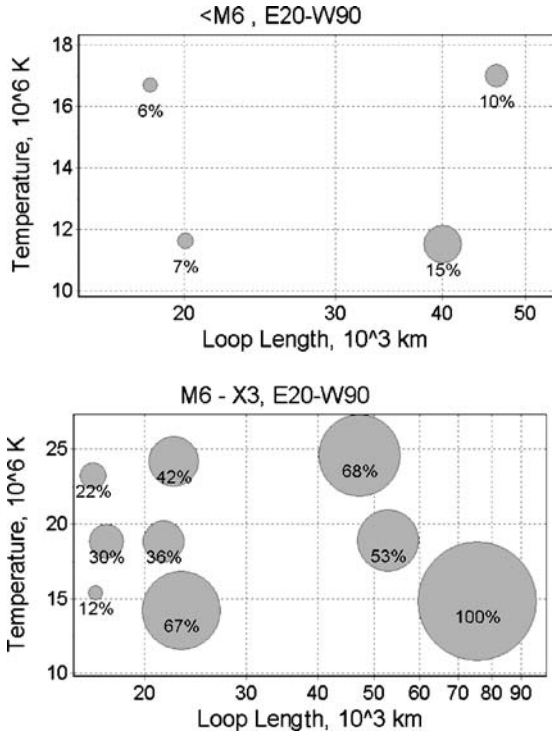

Figure 16. Circle size corresponds with the fraction of the proton flares among the X-ray flares with the different values of temperature and loop length. The *upper panel* represents <M6 flare range and the *bottom panel* gives flares in the M6-X3 range.

three loop length rows, $L < 19$ Mm, $L = 19$–28 Mm and $L > 28$ Mm. The <M6 bin matrix consisted of two temperature columns, $T_m < 14$ MK and $T_m > 14$ MK; and two loop length rows, $L < 28$ Mm and $L > 28$ Mm. Consequently, 9 subsets were selected in the M6-X3 range and 4 subsets in the <M6 range, the latter containing a significantly smaller number of associated SPEs. The dependence of SPE probability on temperature and loop length is depicted in Figure 16.

In each of the flare intensity groups the proton flare fraction is shown to increase with increasing loop size and decreasing temperature; the loop dependence appears to be the more dominant function. For example, all of the 21 flares contained in the 20°E–90°W zone, M6-X3 importance with loop length >60 Mm were followed by SPE while only 12% of the low temperature, <17 MK, compact, ($L < 19$ Mm), flares were SPEs. However, as discussed in the following, the latter result is strongly affected by the large included X-ray intensity range of this grouping that does not discriminate between M6 to X3 flares.

The temperature function expressed by Equation (3–5) (Garcia, 2004a) (see also Garcia, 1994; Garcia, Greer, and Viereck, 1999) is probabilistic and monotonic in both temperature and X-ray intensity. It is further complicated by the facts (1) that

flares naturally trend to higher temperatures with increasing flare intensity, and (2) that near and behind-the-limb flares are apparently (i.e., uncharacteristically) hot (Garcia and McIntosh, 1992); both phenomena are counter-intuitive to an algorithm based on low temperature. At low X-ray intensities (<M3) SPE incidence drops significantly and the low temperature dependence is diminished correspondingly. Thus, computed SPE probabilities at each extreme of the X-ray spectrum depart somewhat from the temperature model and the above formulation and must be modified accordingly.

8. Conclusions

Approximately 1100 near Earth proton events (SPEs) were extracted from 28 years of simultaneous space-based energetic particle and X-ray observations and ground level events (GLEs). This extensive sample of experimental data provided a good basis to study possible links between SPEs and solar flares. Even the most cursory examination of these data reveals a high correlation exists between various parameter combinations. It has been the purpose of this work to explore these correlations in detail to aid in the unraveling of the conundrum bearing on the origins of solar energetic particles: are they the direct product of a flare as originally believed; the result of CME driven shocks, today's preferred interpretation; some combination of both; or does some unrecognized phenomenon underlie the entire process?

The principal findings of this study are summarized as follows:

1. A high correlation exists between the number incidence of SPEs and major (>M5) flares on a scale of months and years.
2. An astonishingly large percentage of SPEs (defined by a less stringent condition than the NOAA SEP criterion) turned out to be associated with individual X-ray flares. Garcia (2004 a,b) suggested that normal flares (i.e., SEPless ≥M1 flares) outnumbered SEP flares by the ratio 40:1.
3. The magnitude of >10 and (>)100 MeV proton enhancements following flares (averaged by the described epoch method) appears to be primarily a function X-ray flare importance and heliographic location. In the longitude interval 15°W–75°W the >10 MeV SPE peak flux dependence on soft X-ray flux follows a power law with exponent 1.14 ± 0.14.
4. The heliolongitude dependence protons from 10 MeV to relativistic energies reveals that many SPEs associate with flares located westward of 70°W, i.e., west of the predominant 45°W–70°W sector.
5. The SPE temporal properties appear to correlate with associated flare's duration, importance and heliographic location.
6. The assumption that the initial proton acceleration occurs at the same time and place as associated flare is not inconsistent with these studies.

7. SPE probability of occurrence increases with the SXR flare duration. This is especially true for the flares of low importance. This correlation becomes less important for more powerful flares, on the prima facie basis that strong flares trend to long duration anyway.
8. The SPE probability of occurrence appears to be inversely related to the maximum temperature and directly related to the loop length of the X-ray flare. These results are in good agreement with Garcia (1994).
9. We anticipate these results may have application to the physics of solar energetic particle generation, as well as to forecasting models concerned with SPE probability of occurrence, time delay and expected proton flux on the basis of the characteristics of the observed X-ray flare.

Acknowledgements

This work is supported by ENTER 2003 70/4/6890 and by Greek Russia Collaboration. Thanks are due to Drs E. Eroshenko, M. Livshits and L. Miroshnichenko for very useful discussions and help in evaluating this paper.

References

Axford, W. L.: 1965, *Planet. Space Sci.* **13**, 1301.
Balch, C. C.: 1999a, *Radiation Measurements* **30**, Elsevier Science, Ltd.
Balch, C. C.: 1999b, Ph.D. thesis, PB2002–101748; NCAR/CT-166.
Bazilevskaya, G. A. and Sladkova, A. I.: 1986, *Geomagnet. Aeronomy* **26**, 187.
Bazilevskaya, G. A., Vashenyuk, E. V., Ishkov, V. N. *et al.* 1983, 1986, *Catalogue of Solar Proton Events 1970–1979*, Yu. I. Logachev (ed.), Moscow, Nauka, IZMIRAN.
Bazilievskaya, G. A., Sladkova, A. I., Fomichev, V. V., and Chertok, I. M.: 1990, *Astronomicheski Zhurnal t.* **67**, 409.
Belov, A., Kurt, V., and Mavromichalaki, H.: 2002, The efficiency of Solar flares with gamma-ray emission of solar cosmic rays production, EGSA.27.5752B.
Belov, A., Kurt, V., Gerontidou, M., and Mavromichalaki, H.: 2001a, *Proc. 27th ICRC,* 3465–3468.
Belov, A. V., Eroshenko, E. A., Oleneva, V. A., and Yanke, V. G.: 2001b, *Proc. 27th ICRC,* Hamburg, **9**, 3552.
Berezhko, E. G., Petukhov, S. I., and Taneev, S. N.: 2001, *Izvestiya RAN, Phys. Series* **64**, 339.
Burkepile, J. T. and St. Cyr, O. C.: 1993, *NCAR Technical Note, NCAR/TN-369+STR*, Boulder, CO.
Burlaga, L.: 1967, *J. Geophys. Res*. **72**, 4449.
Cane, H. V.:1998, *Proc. 25th ICRC*, Durban, **8**, 135C.
Cane, H. V., Reames, D. V., and von Rosenvinge, T. T.: 1988, *J. Geophys. Res*. **93**, 9555.
Cliver, E. W., Reames, D. V., Kahler, S. W. and Cane, H. V.: 1991, *Proc.22nd ICRC*, Dublin, **3**, 25.
Crosby, N. B., Aschwanden, M. J., and Dennis, B. R.: 1993, *Solar Phys*. **143**, 275.
Dorman, L. I. and Miroshnichenko, L. I.: 1968, *Solar Cosmic Rays*, Moscow, Nauka (Fizmatgiz), pp. 468 (in Russian), English edition for NASA by Indian National Scientific Documentation Center, Delhi, 1976.
Feynman, J., *et al.*: 1993, *J. Geophys. Res.* **98**, 13281.

Forbush, S. E.: 1946, *Phys. Rev*. **70**, 771.
Garcia, H. A. and McIntosh, P. S.: 1992, *Solar Phys*. **14**, 109.
Garcia, H. A.: 1994, *Astrophys. J.* **420**, 422.
Garcia, H. A.: 1998, *Astrophys. J.* **504**, 1051.
Garcia, H.: 2000a, *Astrophys. J. Suppl. Series* **27**, 189.
Garcia, H. A.: 2000b, in R. Ramaty and N.Mandzhavidze, (eds.), Quantifying the empirical relationship between loop length and duration of solar flares, High Energy Solar Physics: *Anticipating HESSI, ASP Conf, Ser.*, Vol. 206.
Garcia, H. A.: 2004a, *Space Weather* **2**, SW000001.
Garcia, H. A.: 2004b, *Space Weather* **2**, SW000035.
Garcia, H. A. and Kiplinger, A. L.: 1996, *Proceedings of the 16th International Workshop National Solar Observatory Sacramento Peak*, p. 91.
Garcia, H. A., Farnik, F., and Kiplinger, A. L.: 1998, *Proc. SPIE*, **3442**, 210.
Garcia, H. A., Greer, S., and Viereck, R.: 1999, *Proceedings of the 9th European Meeting on Solar Physics*, ESA SP-448, pp. 983.
Gerontidou, M., Vassilaki, A., Mavromichalaki, H., and Kurt, V.: 2002, *J. Atm. Solar-Terr. Phys.* **64**, 489.
Gombosi, T. I. and Owens, A. J.: 1981, *Adv. Space Res*. **1**, 115.
Gosling, J. T.: 1993, *J. Geophys. Res*. **98**, 18937.
Goswami, J. N., Mc Guire, *et al.*: 1988, *J. Geophys. Res.* **93**, 7195.
Hudson, H. S.: 1995, *EOS Transactions*, AGU, **76**, 405.
Hudson, H. S., Haisch, B. M., and Strong, K. T.: 1995, *J. Geophys. Res*. **100**, 3473.
Jokipii, J. R.: 1971, *Ann. Rev. Astron. Astrophys.* **30**, 9, 1, 27.
Kahler, S. W.: 1992, *Ann. Rev. Astron. Astrophys.* **30**, pp. 113.
Kahler, S. W.: 1993, *J. Geophys. Res*. **98**, 5607.
King, J. H.: 1984, *J. Spacecraft Rockets* **11**, 401.
Krimigis, S. M.: 1965, *J. Geophys. Res*. **70**, 2943.
Kunches, J. M. and Zwickl, R. D.: 1999, *Radiation Measurements 30*, Elsevier, New York.
Kurt, V. G.: 1990, *Basic Plasma Processes on the Sun*, E. R. Priest and V. Krishan (eds.), IAU Symp.142, Kluwer Academic Publishers, The Netherlands, pp. 409.
Kurt, V. G., Mavromichalaki, H. and Gerontidou, M.: 2002, *Proc. "SOLMAG: Magnetic Coupling of the Solar Atmosphere Euroconference and IAU Colloquium 188"*.
Kurt, V., Belov, A., Mavromichalaki, H., and Gerontidou, M.: 2004, *Annales Geophysicae* **22**, 2255.
Livshits, M. A., Badalian, O. G., and Belov, A. V.: 2002, *Astronomy Reports* **46**, 597.
Ma Sung, L. S., van Hollebeke, M. A. I., and McDonald, F. B.: 1975, *Proc. 14th Int. Cosmic Ray Conf*., M (nchen, Germany, **5**, 1767.
Mendoza, B., Melendez, R., Miroschnichenko, L. I., and Perez-Enriquez, R.: 1997, *Proc. 25th ICRC*, **1**, 81.
Miroshnichenko, L. I.: 2001, *Solar Cosmic Rays,* Kluwer Academic Publishers, The Netherlands.
Miroshnichenko, L. I., Mendoza, B., and Perez-Enriquez, B.: 2001, *Solar Phys*. **202**, 151.
NOAA SESC Solar proton Events 2002, *Solar Geophysical Data*, NOAA Boulder CO.
NOAA SESC Solar Proton Events: January 1976–December 1997, Preliminary List: 1998, *Solar-Geophysical Data*, 641, Part II, 30, NOAA, NGDC, Boulder, CO.
Nymmik, R. A.: 1999, *Proc. 26th Int. Cosmic Ray Conf*., Salt Lake City, USA, 6, pp. 268.
Osokin, A. R., Belov, A. V., and Livshits, M. A.: 2003, *Solar System Res.* **37**, 56.
Pearson, D. H., *et al.*: 1989, *Astrophys. J.* **336**, 1050.
Reames, D. V.: 1995, *Revs. Geophys. Suppl*. **33**, 585.
Richter, A. K., Verigin, M. I., Kurt, V. G., *et al.*: 1981, *J Geophys. Res.* **50**, 101.
Ruffolo, D.: 1999, *Astrophys. J.* **515**, 787.

Simnett, G. M.: 2003, International Solar Cycle Studies (ISCS) Symposium, 23–28 June 2003, Tatranská Lomnica, Slovak Republic, A. Wilson (ed.), ESA SP-535, Noordwijk: ESA Publications Division, ISBN 92-9092-845-X, pp. 613.

Shea, M. A.: 1990, *Proc. 21st Int. Cosmic Ray Conf., Invited Papers, Highlight Papers, Miscellaneous*, Adelaide, Australia, 12, pp. 196.

Shea, M. A. and Smart, D. F.: 1990, *Solar Phys.* **127**, 297.

Shea, M. A. and Smart, D. F.: 2000, *Space Sci. Rev.* **93**, 187.

Sladkova, A. I., Basilevskaya, G. A., Ishkov, V. N. *et al.*: 1990, Y. I. Logachev (ed.), *Catalogue of Solar Proton Events 1980–1986*, Moscow University Press.

Sladkova, A. I., Bazilevskaya, G. A., Ishkov, V. N. *et al.*: 1998, Y. I. Logachev (ed.), *Catalogue of Solar Proton Events 1987–1996*, Moscow University Press.

Van Hollebeke, M. A., Wang, J. R., and McDonald, F. B.: 1974, X-661-74-27, NASA Goddard Space Flight Center.

Van Hollebeke, M. A. I., Ma Sung, L. S., and Mc Donald, F.: 1975, *Solar Phys.* **41**, 189.

Vestrand, W. T., Chare, G. H., Murphy, R. J., Forrest, D. J., Rieger, E., Chupp, E. L., and Kanbach, C.: 1999, *Astrophys. J. Suppl. Ser.* **120**, 409.